

THE FLUCTUATIONS IN THE IRAS DISTRIBUTION

R.B. Shatsova, G.B. Anisimova

Rostov Pedagogical University, *galina@iubip.ru*

ABSTRACT. The great fluctuations in the infrared sky are situated along the meridians of Universal Sky Net.

It is related also to the large structures. So the edge of the zone of avoidance of galaxies over IRAS₆₀ and IRAS₁₀₀ for long extension coincides to the Γ meridian, perpendicular to the ecliptic E. The Large Magellanic Cloud is situated near the southern pole of ecliptic. The IR radiation of the zodiacal belt, discovered by Hauser, is confirmed. Perhaps, it is obliged not only and not so much to a zodiacal light of the Solar system.

Key words: IRAS, structure of Galaxy, Universal Sky Net.

One can distinguish both regular and accidental components in the distributions of stellar and nonstellar matter. The concentrations to the plane and to the centre of Galaxy, to the Gould Belt and others are considered as the regular ones. And the deflexions from them are attributed to the accidental fluctuations.

The fluctuations, which own the certain predicted characteristics, must be excluded from the number of accidental ones. Such predictions give, in particular, the regular multi-polar Universal Sky Net (USN). A lot of its poles are the known in astronomy points. Every C-pole has the intersection of its own bunch of meridians. There are known in astronomy circles among them.

USN permits to join almost all well known in astronomy elements into the united net and to find the regularities in their mutual orientation.

USN is built on the basis of:

1. One of known circles (for instance, ecliptic – E)
2. The fastened point (for instance, η - the intersection of ecliptic E with the Galactic equator – MW)
3. The net is branching in the poles by the empiric rule

The common USN geometry was described in (Shatsova & Anisimova, 2003; 2004). The used in this article net elements (the bunches of meridians in ξ , η , ζ poles), are shown in Fig. 1, 2 and Table 1.

The equation for k- meridian of the bunch in C-pole is presented in the used here polar coordinate system (Ω , ρ):

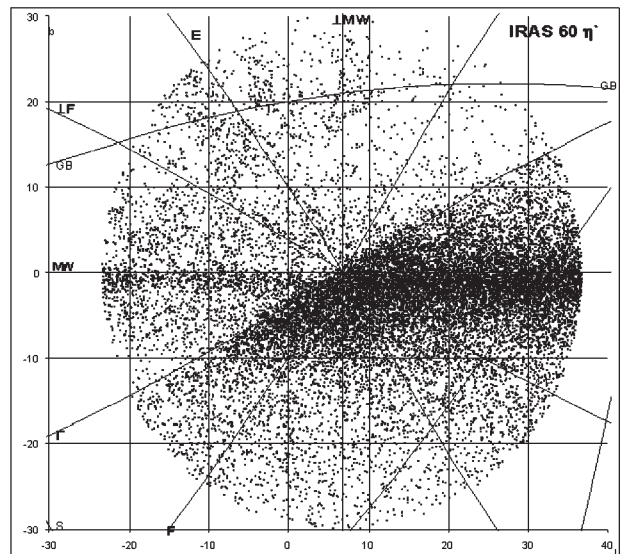


Figure 1: The position of IRAS sources $\lambda = 60\mu m$ in the pole η and the USN meridians

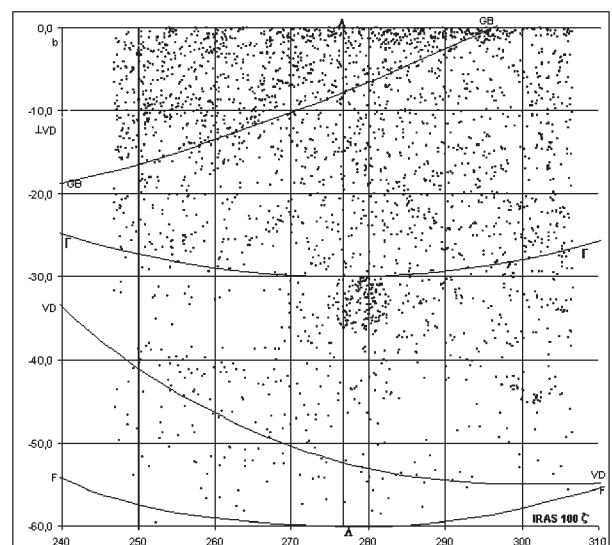


Figure 2: The position of IRAS sources $\lambda = 60\mu m$ in the pole ζ and the USN meridians

Pole	Meridians			Pole	Meridians			Pole	Meridians		
ξ	k	sym- bol	Ω	η	k	sym- bol	Ω	ζ	k	sym- bol	Ω
m=4	0	Λ	0°	m=6	0	\perp MW	0	m=2	0	Λ	0
$l=96.7^\circ$	1	S	45°	$l=186.7$	1	E	30	$l=96.7$	1	Γ	90
$b=-60^\circ$	2	E	90°	$b=0^\circ$	2	\perp F	60	$b=30^\circ$			
	3	\perp Γ	135		3	MW	90				
$\lambda=0^\circ$				$\lambda=90^\circ$	4	Γ	120	$\lambda=0^\circ$			
$\beta=0^\circ$				$\beta=0^\circ$	5	F	150	$\beta=90^\circ$			

Table 1: The USN elements are presented: the poles - coordinates (galactic-(l, b) and ecliptical-(λ, β)), and the number of meridians, intersecting in this poles (m); the meridians - the symbol and the positional angle Ω of each meridian

$$\Omega_C = \Omega_0 + k\pi/m_C, \quad (1)$$

where $k=0, 1, \dots, m_C - 1$, m_C - the number of meridians in the bunch: $m_\xi=4$, $m_\eta=6$, $m_\zeta=2$.

The positional angle Ω is measured off the direction to the North Galactic Pole Π_{MW} to the side of increase of galactic longitudes l , ρ - the radius-vector or the angular polar distance along the great circle.

In this work we examined the IRAS data (IRAS Point Source Catalog, 1985) in two waves (60 and 100 μ) in classes 2 and 3 in the sky regions around (ξ, η, ζ) poles in radius 30° and the opposite poles (ξ', η', ζ'), that is about 40% of the sky. The IR radiation is connected with the dust shells of the stars, nebulae and the galaxies.

Each element of USN has not only the geometrical sense, but also reflects some peculiarities of cosmic structures.

The two examples over the IRAS data is shown here.

1. IRAS₆₀ in the region of η' pole, situated near the centre of the Galaxy ($l=0^\circ$, $b=0^\circ$), (Fig.1).

The meridians Γ , MW and E are very clearly seen here. The great circle Γ passes through the celestial and ecliptic poles, and the solstices. The IR map shows a triangle of very dense dust. Γ is exactly its hypotenuse for the length of tens degrees. The optical map shows, that this line is the edge of the zone of avoidance of galaxies (de Vaucouleurs, 1959). The MW meridian passes along the radius of the region along the northern edge of the narrower dense galactic zone. The E meridian outlines the right edge of the zodiacal IRAS concentration.

It is remarkable, that the edge's lines coincide the meridians, and their intersection - η' pole of USN.

The edge locations form the effect of density asymmetry. The Γ and E sides of lower density are turned to the I quadrant, and of higher density are turned to the III quadrant. The quadrants have no symmetry relatively MW, moreover, MW zones raise the density in II and IV quadrants. Hence it follows the density asymmetry around the pole itself. So MW and Γ meridians are at the edges of large-scale structures. And E, F,

\perp F and \perp MW are at the edges of smaller density fluctuations.

The connection of IRAS distribution with the USN net is the sign of regularity and, hence, it is not accidental.

2. IRAS₁₀₀ in the region of the southern ecliptical pole - ζ' (Fig. 2)

Only two USN circles intersect here - Γ and Λ . Λ also passes through the galactic poles. Large Magellanic Cloud (LMC), having strong IR radiation, is near this pole. Γ and Λ touch the core of LMC. The internal LMC structures are parallel to Γ and Λ (Efremov, 1989, Fig. 21). The bright LMC halo asymmetrically surrounds ζ' , but there is larger ($\approx 10^\circ$) and more symmetrical to ζ' circle - the parallel to E near the pole. We see the density jumps on Γ , Λ and especially on GB (Gould Belt), creating the asymmetry of density in the quadrants.

These and other poles are situated in the centers of chosen regions, within $\rho=30^\circ$. It is natural to examine the distribution of point IRAS sources in polar coordinates (Ω, ρ). The coordinates (Ω, ρ) can be obtained from (l, b):

$$\begin{aligned} tg\Omega &= \frac{\sec b_c \cdot \sin(l-l_c)}{tg b - tg b_c \cdot \cos(l-l_c)} \\ \sin \rho &= \frac{\cos b}{\sin \Omega} \cdot \sin(l-l_c) \end{aligned} \quad (2),$$

where (l_c, b_c) - the coordinates of C pole (see Table 1).

The polar net is divided into the cells S_i ($\Delta\Omega=5^\circ$, $\Delta\rho=5^\circ$). The object numbers n_i and the corresponding density - $d_i = n_i/S_i$ are counted in each cell.

As we examine the accidental components, we must exclude from d_i the regular component - the mean $d(b)$ in the region at latitude b , that reflects first of all the galactic concentration. For each region and each IRAS wave length we obtained the histograms of $\Delta d_i = d_i - d$ in the cells of sectors in function of Ω (or a symbol of meridian) for each interval of ρ_j . There are positive and negative deflexions.

The example for the region of η pole, IRAS₁₀₀ is presented in Fig.3.

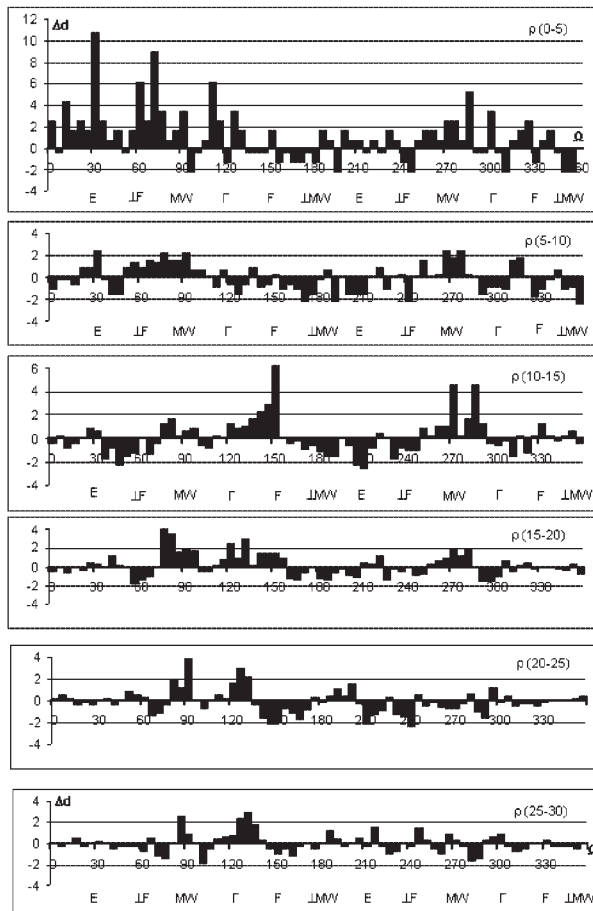


Figure 3: The example of Δd histogram for different ρ intervals around the η - pole for IRAS₁₀₀

Δd depends systematically on Ω . The largest density jump from $\Omega(0-130^\circ)$ sector to $\Omega(130-250^\circ)$ sector is seen near the pole, at $\rho=0-5^\circ$. The density jumps from $\Delta d > 0$ to $\Delta d < 0$ reduce at the other ρ , the sector borders varies slightly, but the contrast is remained. The $\Delta d > 0$ peaks, as a rule, lie at the meridians, and $\Delta d < 0$ corresponds to the space between the meridians.

Fig. 4 shows the examples of the combined histograms. For compactness, $\Delta d(\rho_j)$ are presented for different ρ_j at every Ω in each histogram, but it does not mean the summing up.

The largest fluctuations along the meridians, corresponding Ω_i and Ω_i+180 in all divisions of the material are given in Table 2, where $\Delta d_{max}(\Omega)$ is the density excess and in brackets (N) – the number of cells, having $\Delta d > 0$.

The joint analysis of Fig. 3-4 and Table 2 confirms the conclusions, obtained from Fig. 1-2 analysis. But, the numerical comparison can be done only inside the same region. And than one can do the qualitative comparison between the different regions.

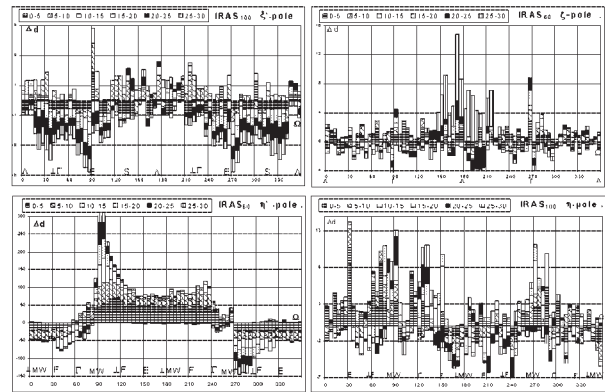


Figure 4: The examples of IRAS Δd histograms in function (Ω, ρ)

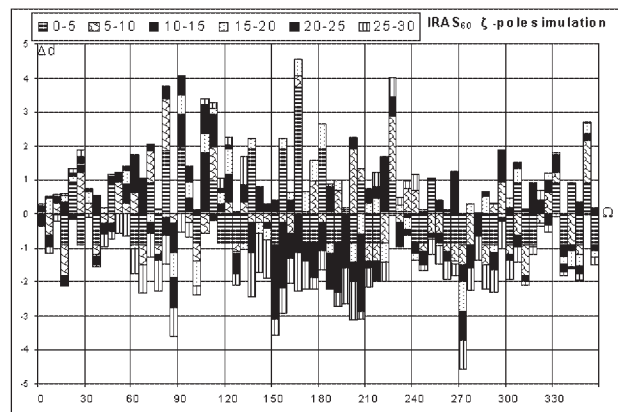


Figure 5: The distribution of density excess (Ω, ρ) for IRAS simulation $\lambda = 60m\mu$ in the ζ -pole

Table 2 shows the connection of the density fluctuations with the majority of the USN meridians. Hence, the interpretation given by Hauser (1995) as a zodiacal light of the Solar system is doubtful. It was obtained in particular over IRAS₁₂ and IRAS₂₅ data for one meridian – E. The connection of USN with the galactic and extragalactic structures was discussed in (Shatsova & Anisimova, 2004).

We made the accidental simulations in conditions of galactic concentration. The number of points, equal the number of real objects were scattered accidentally inside each zone on latitude $\Delta b=10^\circ$. The (Ω, ρ) distribution was obtained over the same procedure as for the real objects. There is no peculiarities in the simulated distribution, only the MW concentration and the peculiarity of the formula (2) $tg\Omega = \infty$, for $\Omega=90, 270$. The example is shown in Fig. 5.

The main conclusions:

1. It is confirmed the predicted by USN the similar regularity in the distribution of fluctuations and large-scale structures: the density excess along the meridians and its deficit between the meridians and near the net's

Table 2: Maximal deflections of IRAS density from mean density

	IRAS 60						IRAS 100						
	Λ	$\perp\Gamma$	E	S	$\parallel(S)$		Λ	$\perp\Gamma$	E	S	$\parallel(S)$		
ξ	1,2 (7)	2,1 (3)	2,1 (5)	1,9 (5)	4 (5)		1,2 (6)	1,1 (3)	2,0 (3)	1,9 (4)	3,9 (5)		
ξ'	2,0 (7)	1,9 (5)	2,0 (6)	0,6 (6)			1,7 (7)	1,9 (5)	1,9 (6)	1,6 (5)			
	$\perp MW$	E	$\perp F$	MW	Γ	F	$\perp MW$	E	$\perp F$	MW	Γ	F	$\parallel(\Gamma)$
η	4 (6)	8 (5)	11 (5)	8 (11)	8 (8)	6 (7)	4,5 (6)	11 (7)	9 (6)	4,5 (11)	6 (7)	6 (7)	5,5 (3)
η'	50 (4)	50 (4)	75 (5)	60 (6)	45 (7)	50 (3)	50 (4)	50 (3)	70 (5)	60 (6)	45 (4)	70 (4)	
	Λ	$\perp\Gamma$	LMC		MW	GB	Λ	$\perp\Gamma$	LMC		MW	GB	
ζ	10 (9)	3 (10)			5,5 (5)		7 (7)	3,4 (9)			5 (8)		
ζ'	13 (6)	16 (5)	20 (5)		4,4 (4)	5,0 (4)	12 (7)	6,8 (7)	12,5 (5)			2,5 (4)	

poles. The existence of unknown before meridians F, $\perp F$, $\perp\Gamma$ and S is confirmed over these features.

2. It is noticed the unknown peculiarities of the USN elements: the meridians and the poles are situated at the edges of sky belts, where the density jumps take place. This asymmetry leads to the division of the space into the sectors of different density.

3. The connection of the majority of IRAS fluctuations and the USN elements means that the fluctuations of density are not accidental. The same follows from the obtained simulations.

4. There is no qualitative differences for IRAS₆₀ and IRAS₁₀₀ distribution, only in details.

As the positive fluctuations along the meridians and the negative between them were predicted, then the observed such fluctuations are not accidental.

References

- Shatsova R.B., Anisimova G.B.: 2003, *Astrofizika*, **46**, 319.
 Shatsova R.B., Anisimova G.B.: 2004, *IRAS Point Source Catalog, Washington*, 1985.
 G. de Vaucouleurs: 1959, *Soviet Astron Zh*, **36**, 977.
 Efremov Y.N.: 1989, *Sites of star formation in galaxies*.
 Hauser M.G.: 1995, *IAU Sympos*, **168**.